Korean Journal of Remote Sensing, Vol.20, No.1, 2004, pp.47~55

Brightness Temperature Retrieval using Direct Broadcast Data from the Passive Microwave Imager on Aqua Satellite

Seung-Bum Kim*, Yong-Jo Im*, Kum-Lan Kim, Hye-Sook Park**, and Sung-Ok Park***

Satellite Technology Research Center, Korea Advanced Inst. Science and Tech.*

Korea Meteorological Administration**

Abstract : We have constructed a level-1 processor to generate brightness temperatures using the direct-broadcast data from the passive microwave radiometer onboard Aqua satellite. Although 50-minute half-orbit data, called a granule, are being routinely produced by global data centers, to our knowledge, this is the first attempt to process 10-minute long direct-broadcast (DB) data. We found that the processor designed for a granule needs modification to apply to the DB data. The modification includes the correction to path number, the selection of land mask and the manipulation of dummy scans. Pixel-to-pixel comparison with a reference indicates the difference in brightness temperature of about 0.2 K rms and less than 0.05 K mean. The difference comes from the different length of data between 50-minute granule and about 10-minute DB data. In detail, due to the short data length, DB data do not always have correct cold sky mirror count. The DB processing system is automated to enable the near-real time generation of brightness temperatures within 5 minutes after downlink. Through this work, we would be able to enhance the use of AMSR-E data, thus serving the objective of direct-broadcast.

Key Words : AMSR-E, Aqua, Passive Microwave Sensor, Direct Broadcast.

1. Introduction

Aqua is a major satellite mission of the Earth Observing System (EOS), an international program centered at the U.S. National Aeronautics and Space Administration (NASA). The Aqua satellite carries six distinct earth-observing instruments to measure numerous aspects of earth's atmosphere, land, oceans, biosphere, and cryosphere, with a primary objective of monitoring the water cycle of the Earth. This objective is established to examine whether the water cycle of the earth is accelerating, e.g., more rain and evaporation. Launched on May 4, 2002, the satellite is in a sun-synchronous orbit at an altitude of 705 km, with a track that takes it north across the equator at 1:30 P.M.. Aqua provides a direct broadcast (DB) to local users, meaning the direct transmission of data from the satellite to local ground stations.

Among the six sensors onboard Aqua satellite, in this paper we describe the processing of AMSR-E

Received 15 September 2003; Accepted 26 January 2004.

(Advanced Microwave Scanning Radiometer for EOS) data. AMSR-E is a six-frequency dual-polarized total-power passive microwave radiometer with the frequency ranging from 6.9 to 89 GHz (Kawanishi *et al.*, 2003; Table 1). It provides numerous water-related geophysical parameters such as sea surface temperature, soil moisture, precipitation rate, water vapor, cloud liquid water and sea ice coverage (Wilheit and Chang, 1980).

For the first time among the direct broadcast community of AMSR-E, we have established the DB system for generating brightness temperatures (T_b). Our system is based on ADS (AMSR Data processing Software), developed by Japan's JAXA (Japan Aerospace Exploration Agency). ADS was released to the public in June 2003 after 1-year of sensor verification. ADS is designed to process 50-minute data, while the DB data are about 10-minute long. Consequently, only the 50-minute data are distributed through a few data centers in the world at present. Thus the merit of DB is not fully exploited. In this paper we present (1) how to adapt ADS to process the DB data, (2) our automated system for producing AMSR-E T_b, (3) the performance assessment of our system and (4) the sample generation of level 2 products.

2. System Overview

The AMSR-E processing system is detailed in Fig. 1. The direct-receiving station receives data from Aqua

Table 1. Specification of AMSR-E.

Orbit (km)	705 (sunsynchronous, ±82 latitude)					
Repeat cycle (day)	16					
Swath (km)	1450					
Center Frequencies (GHz)	6.9	10.7	18.7	23.8	36.5	89.0
Resolution (km (km)	75×43	51×29	27×16	32×18	14×8	6×4
Sampling Rate (km x km)	10×10	10×10	10×10	10×10	10×10	5×5
NE(T (K)	0.3	0.7	0.7	0.7	0.6	1.2
Data size / scene (MB)	21 (including all channels & levels to L1B)					

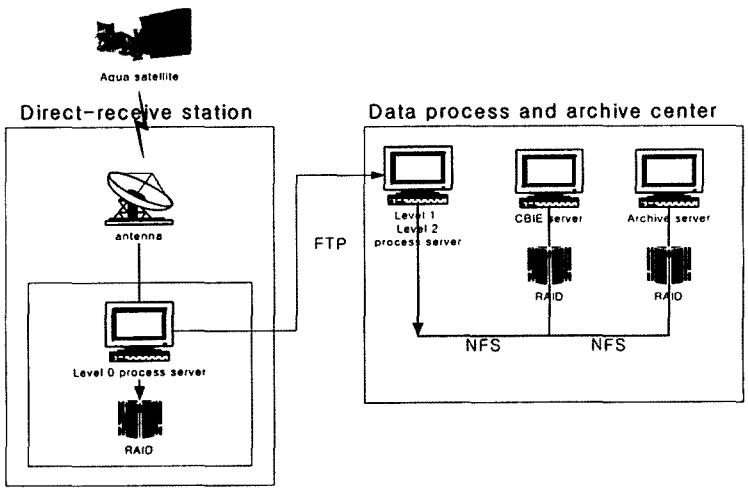

Fig. 1. Overview of Aqua direct-broadcast and the level 0-2 processing system. CBIE stands for "Catalogue and Browse Image Extraction".

satellite and converts the raw data strip to level-0 PDS (production data set). In this work, we developed a level-1 processor based on JAXA's ADS to produce T_b from the L0 PDS. Different levels are defined in Fig. 2 and Table 2. The L0 data are transmitted by FTP. The arrival of L0 data initiates the L1 processor. Upon the completion of L1 generation, level-2 processors are executed. The L1 and L2 data are sent by NFS to the catalogue and browse system and the archive server. All these processes run automatically by the arrival of L0 data. It takes less than 5 minutes on SGI Octane machine to generate L1 and L2 data from one PDS file. An error may occur during the automatic processes and also a human operator may wish to run L1 or L2 processor semi-automatically. Our system supports such manual intervention. Fig. 3 illustrates the automatic/ semi-automatic scenarios of operation, and defines the interface between components.

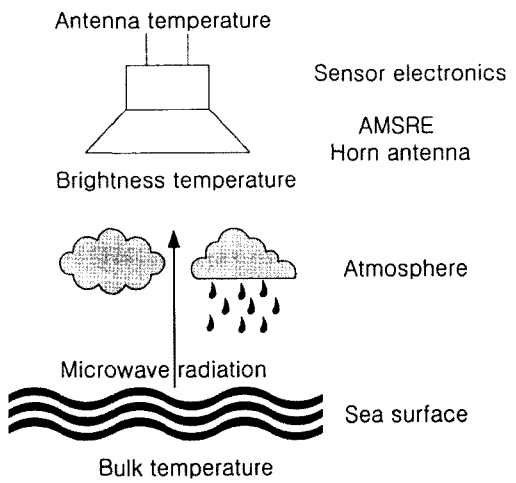

Fig. 2. Illustration of data levels for passive microwave remote sensing.

3. Brightness Temperature Retrieval

The L1 processor produces T_b and is composed of radiometric calibration and geolocation units. The radiometric calibration converts observational counts to antenna temperatures (T_A):

$$T_A = \text{slope}*\text{digital count} + \text{offset},$$

where *digital count* is the quantized reading by the electronics of the Earth's radiation. *Slope* and *offset* are determined by onboard calibrators (Fig. 4 and Fig. 5). To convert the antenna temperature to T_b, cross-polarization (cross-polarized energy received by a desired port) and spill-over effects need to be corrected. The cross-polarization is modeled as

$$T_{bv} = A_{vv} T_{Av} + A_{hv} T_{Ah} + A_{ov} \quad (1).$$
$$T_{bh} = A_{hh} T_{Ah} + A_{vh} T_{Av} + A_{ov}$$

A_{vv} and A_{hh} are the co-polarization coefficients (~ 1.03 for 6.9 GHz, pre-defined), A_{vh} and A_{hv} are the cross-polarization coefficients (~ -0.03 for 6.9 GHz), and A_{ov} is the background radiation.

The geolocation comprises several coordinate transformation steps from the sensor coordinate to the

Table 2. Definition of different data levels.

Level	Definition
Level 0	Packets of data received from satellite: science data and ancillary data.
Level 1A	L1A data contain observation counts that are the digital numbers of feed horn voltage. L1A data have been geolocated and include regression coefficients for radiometric calibration.
Level 1B	Radiometric calibration converts observational counts to antenna temperature. Furthermore, by correcting for cross-polarization and antenna spillover, the antenna temperature becomes brightness temperature.
Level 2	L2 data are the water related physical parameters (accumulated water vapor, accumulated cloud liquid water, amount of precipitation, sea surface wind speed, sea surface temperature, sea ice concentration, snow water equivalence, and soil moisture) calculated from L1B data.

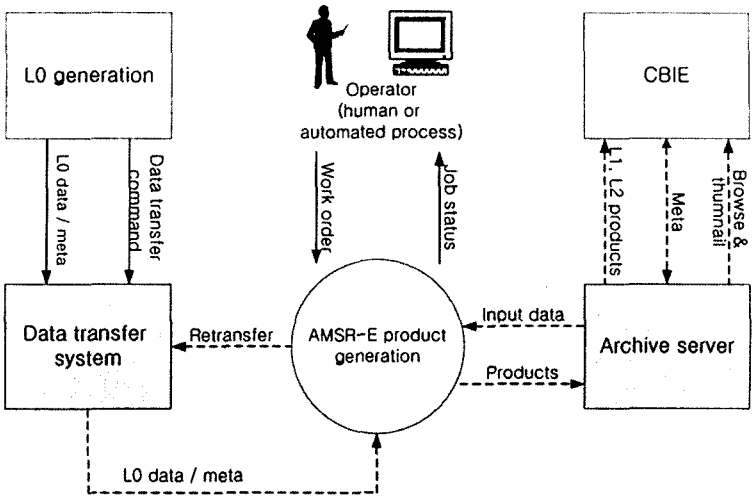

Fig. 3. Operation environment for AMSR-E.

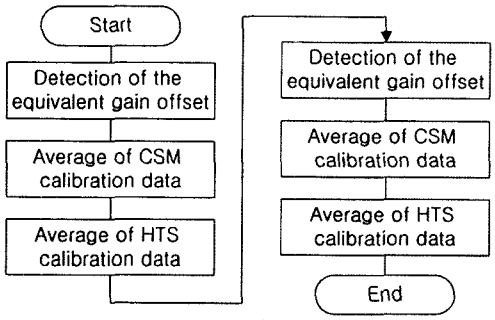

Fig. 4. Block diagram of radiometric calibration. The cold sky mirror (CSM) and the hot temperature source (HTS) are two temperature references for the radiometric calibration. Courtesy: JAXA.

ECR (Earth-Centered-Reference). The ancillary data and the precise time information are needed additionally to assign coordinates to each pixel.

The consequent T_b values are shown in Fig. 6 as an example. Only three channels are selected as examples. Also we choose to show vertical polarization since higher emissivity than horizontal polarization offers better contrast among different features. Cirrus and cumulus clouds appear in high-frequency band but become transparent as the wavelength increases (6.9

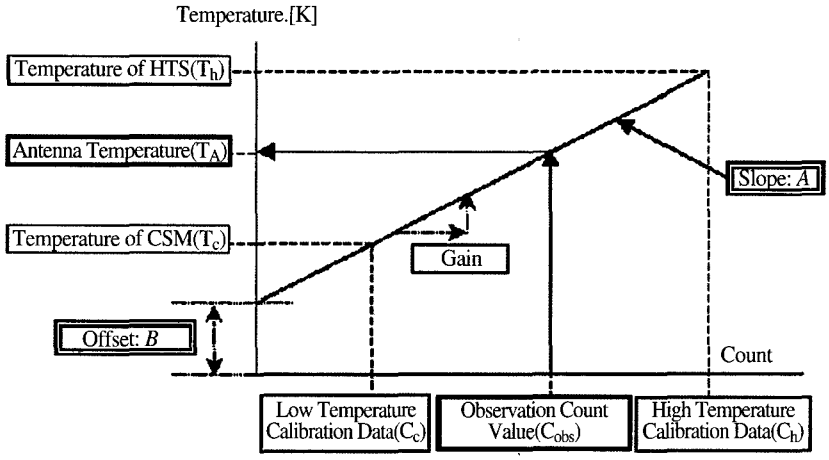

Fig. 5. Radiometric correction: conversion from observational digital counts to antenna temperatures. Courtesy: JAXA.

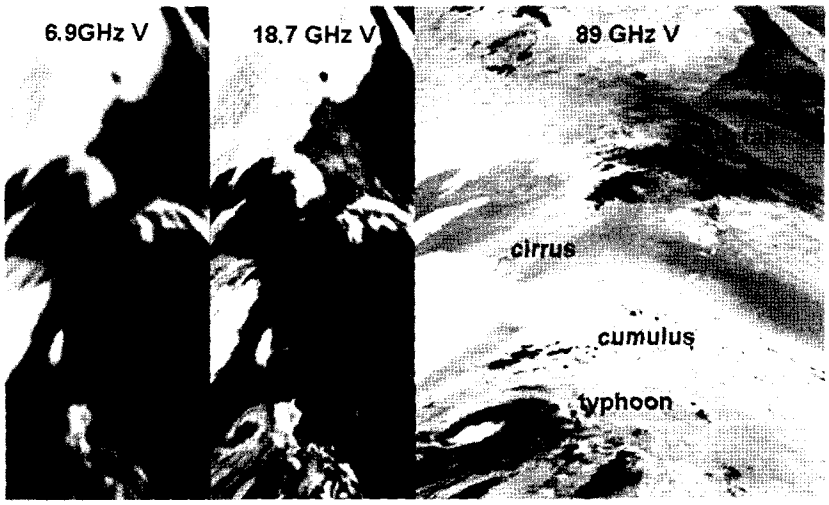

Fig. 6. Examples of multi-channel AMSR-E data. The scene date is 20030722 on path 115.

GHz). 6.9 GHz demonstrates the advantage of a microwave sensing of surface properties, such as sea surface temperature, in that we may avoid clouds contamination. We may identify the rain cells west off Philippines and in the East Sea, even in 6.9 GHz. This is because of the emission during the condensation. The spatial resolution in along-track direction is 75 km, 27 km and 6 km for 6 GHz, 18 GHz and 89 GHz, respectively. The different resolution defines the sharpness of the coastline.

4. Processing of Direct-broadcast Data

Our environment for T_b retrieval differs from the JAXA's system in many respects. These differences are listed in Table 3. Due to these differences JAXA's ADS fails to process DB data. In this work, we have modified the JAXA ADS and here are some important details.

- Most important difference is the length of data. JAXA's data are received by the EOS ground stations near the north pole, and therefore they can receive a granule (half-orbit data). However, local ground stations can collect only overpass data, which are about 10-minute long.
- AMSR-E path number changes when Aqua crosses the equator in an ascending track. Since a

Fig. 7. Images showing the impact of dummy scans at the scene start (bottom). Date of the scene is 20030808 on path 221.

Table 3. Differences between our system and JAXA' s system.

	JAXA system	Our system
Data length (L0, L1)	A granule (50 mins)	6-12 mins
Data distribution (L1)	By JAXA and NSIDC	Local direct-receive station
CSM correction	Available	Not available
Landmask	Need to modify ADS to process direct-broadcast data.	
Dummy scan		
Path numbering		

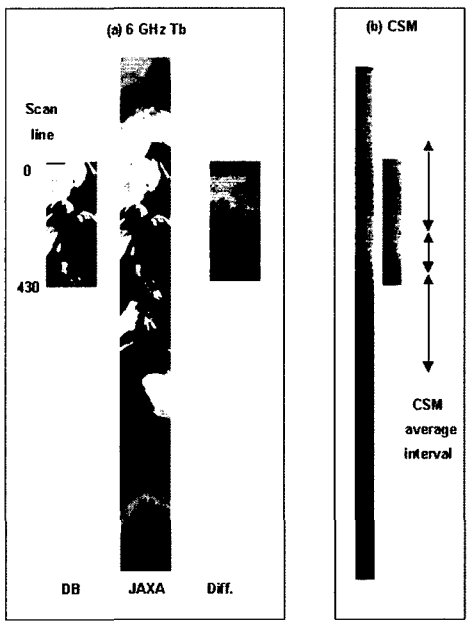

Fig. 8. Analysis of the difference in Tb between DB and JAXA data for a descending scene (the scan begins in the north).

50-min granule covers from pole to pole, for an ascending scene, the path number changes inside a granule. This rule makes the same scene over Korea acquire different path numbers between DB and JAXA products. Since landmask is selected using a path number in ADS, the path number error leads to a wrong landmask. We have modified ADS to make two path numbers the same.

- Data quality at the beginning of data reception from a satellite is dubious because the matching between satellite antenna and ground antenna may be incomplete. This generates dummy garbage data at the scene start (Fig. 7).. JAXA's ADS does not consider this situation since it is designed to process 50-minute long data. We have modified ADS to avoid this 'dummy scan error'.

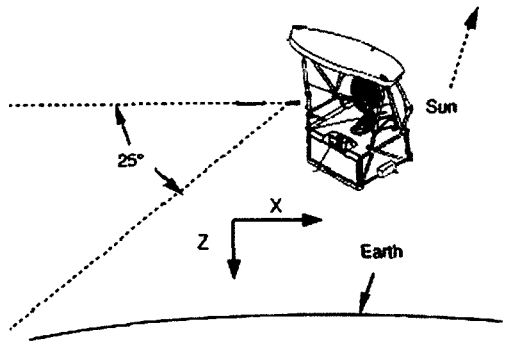

Fig. 9. Geometry of CSM observation of the background radiation. Satellite proceeds in +x direction and the CSM observes backward within the 25° window.

Table 4. Pixel-to-pixel validation with JAXA L1B product. The date of the scene is 20030722 on path 204. Units are digital number for L1A and Kelvin for L1B brightness temperature.

Channel	DB - JAXA			
	stdev	mean	max	min
6V T_b (L1B)	0.15	-0.03	0.5	-0.3
6V Observation count (L1A)	0	0	0	0
10V T_b (L1B)	0.15	-0.06	0.3	-0.5
18V T_b (L1B)	0.24	-0.02	0.6	-0.5
23V T_b (L1B)	0.20	-0.02	0.4	-0.4
36V T_b (L1B)	0.09	-0.05	0.2	-0.4
89BV T_b (L1B)	0.15	-0.04	0.4	-0.4

5. Verification of Direct-broadcast Data

To examine whether our T_b matches the JAXA's standard product, we have performed pixel-to-pixel verification with JAXA L1B product as a reference. The verification results in Table 4 indicate the difference in T_b of about 0.2 K r.m.s and less than 0.05 K mean. To understand this differences, let us examine its spatial map in Fig. 8a. There are two features in the map: (1) the gradient in the difference w.r.t. the scanline, *i.e.*, in alongtrack direction and (2) the shape of the Earth appearing in the difference.

Regarding the gradient in the difference, we have identified two causes. It is important to note that the disagreement develops entirely from the radiometric calibration to obtain T_A. This attribution is supported by the perfect agreement in the observation counts (L1A) between DB and JAXA products (Table 4) The two causes are:

- First of all, the correct values from the cold sky mirror (CSM) are not available in DB data since correct CSM data at a given time are taken 115 scans back, due to the viewing geometry (Fig. 9). In this absence of CSM data, ADS uses a default value. As a result the CSM calibration values (T_c and C_c in Fig. 5) will be different between DB and JAXA data. This error exists only from scanline 0 to scanline 115. The use of the default CSM values produces about 0.7 K error over the ocean, and 1 K error over the land (Imaoka *et al.*, 2003).
- Secondly, the calibration data (T_c and C_c and T_h and C_h, in Fig. 4) from the two on-board calibrators, namely HTS (hot temperature source) and CSM, are averaged in time, *i.e.*, alongtrack. The averaging interval in alongtrack is the same between DB and JAXA data. However, since DB data are shorter, the number of HTS/CSM data used during the average will be less with DB data than with JAXA data (see Fig. 9b for illustration). This results in Tb differences near the two edges of the DB scene.
- The above two attributions concern the discrepancy near the scene edges. For the gradient pattern at the center of the difference map, further calibration algorithms appear to be responsible (T. Takeshima, personal communication) but detailed investigation is needed.

As to the shape of the Earth found in the difference, this would arise when the size of the difference is proportional to the size of T_b.

6. Retrieval of a Level-2 Parameter

To demonstrate that AMSR-E can offer useful geophysical parameters, we have retrieved sea surface temperature (SST). Microwave radiation below 10 GHz is more sensitive to SST changes than other frequencies (Fig. 10) and therefore we use 6.9 GHz. In fact, one of AMSR-E's merits is 6.9 GHz and the consequent retrieval of SST and soil moisture. We further prefer vertical-polarization data because at 55° incidence angle the vertical polarization offers higher emissivity.

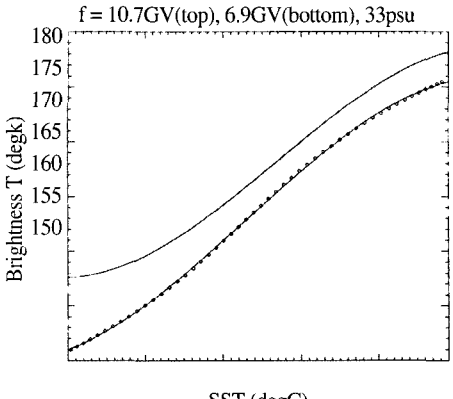

Fig. 10. Sensitivity of emissivity (e, $T_b = e$ * SST) in 10.7 GHz and 6.9 GHz frequencies at 55° incidence angle and 33.0 p.s.u. (practical salinity unit).

Emissivity for vertical polarization (e_v) is given as

$$e_v = 1 - \left| \frac{\varepsilon \cos i - \sqrt{\varepsilon - \sin^2 i}}{\varepsilon \cos i + \sqrt{\varepsilon - \sin^2 i}} \right|^2, \quad (2)$$

where ε is the dielectric constant of sea water and is a function of frequency, salinity, and temperature. i is the incidence angle. One may refer to Wentz (2000) for more details of SST retrieval. The sample SST in Fig. 11 appears reasonable for July. Nonetheless the SST retrieval is far from complete and we need to correct the following overestimation. In the rain cases, the latent heat released during condensation produces additional radiation. Thus in Fig. 11, SST is saturated over rainy areas. Also, the wind generally increases radiation as the water surface area enlarges. Finally, along the coast there is contamination due to the emission by land mainly because the size of AMSR-E's footprint is 75 km × 43 km. Such contamination may be eliminated based on the point distribution criteria with the points being land pixels at higher spatial resolution (Kim, 2004).

Fig. 11. Pseudo-colored SST from AMSR-E 6.9 GHz for a scene shown in Fig. 6. The coastline appears smeared because of the low spatial resolution (43 × 75 km).

SSM/I (Special Sensor Microwave/Imager since 1987) and MSMR (Multi-frequency Scanning Microwave Radiometer, launched on 1999) have also been used for SST retrieval. The major advance of AMSR-E from SSM/I is the addition of a low frequency channel, 6.9 GHz. With this addition, AMSR-E is expected to provide accurate estimates of sea surface temperature and soil moisture. MSMR has a 6.9 GHz channel but it lacks high frequency channels that are needed to correct for the rain and wind effects. Also AMSR-E has better radiometric sensitivity than MSMR by a factor of two as well as higher spatial resolution. In view of these differences, AMSR-E SST is expected to be more accurate than MSMR SST.

7. Conclusions

We have constructed a level-1 processor to generate brightness temperatures, for the first time, using the DB data from AMSR-E. Modification of JAXA's processor, which is designed for handling 50-minute granule, is necessary to manipulate the DB data that are about 10-minute long. We have implemented the necessary modification that includes the correction to path numbers, the selection of land mask and the processing of dummy scans. Pixel-to-pixel verification exhibits our system performs well. The DB processing system is automated to enable the near-real time retrieval of brightness temperatures. Through this work we would

be able to enhance the use of AMSR-E data, thus serving the objective of direct-broadcast. Finally by combining the data from other sensors on Aqua satellite, we may be able to study the Earth's water cycle more effectively. For this end, we plan to use the data from the Aqua's infrared sounding suite (Kim *et al.*, 2003).

Acknowledgements

We are very grateful to Dr. Takeshima for the valuable discussions on AMSR-E data analysis and to Dr. Shibata for suggestions on SST. We thank also JiHyun Shin, MoonGyu Kim, JongJu Lee and SeungHwan Park for important assistance, and manuscript reviewers for their comments. JAXA and NSIDC are acknowledged for providing ADS. This work is supported by the Korea Meteorological Administration.

References

Imaoka, K., Y. Fujimoto, M. Kachi, T. Takeshima, K. Shiomi, H. Mikai, T. Mutoh, M. Yoshikawa, and A. Shibata, 2003. Post-launch calibration and data evaluation of AMSR-E, *Proc. IEEE Geosc. Remote Sens.*, Toulouse, in CD-ROM.

Kawanishi, T., T. Sezai, Y. Ito, K. Imaoka, T. Takeshima, Y. Ishido, A. Shibata, M. Miura, H. Inahata, R. W. Spencer, 2003. The Advanced Microwave Scanning Radiometer for the Earth Observing System (AMSR-E), NASDA's contribution to the EOS for global energy and water cycle studies, *IEEE Trans. Geosci. Remote Sens.*, 41:184-194.

Kim, S. B., 2004. Eliminating extrapolation using point distribution criteria in scattered data interpolation, *Computer Vision and Image Understanding*, in press, doi:10.1016/j.cviu.2003.12.001.

Kim, S. B., H. S. Park, K. L. Kim, S. H. Park, M. G. Kim, and J. J. Lee, 2003. Preprocessing of the direct-broadcast data from the Atmospheric Infrared Sounder (AIRS) sounding suite on Aqua satellite. *Atmosphere*, 13:71-79.

Wentz, F. 2000. Algorithm Theoretical Basis Document (ATBD) AMSR ocean algorithms. RSS Technical Proposal, 121599A-1, 74p.

Wilheit, T. T. and A. T. C. Chang, 1980. An algorithm for retrieval of ocean surface and atmospheric parameters from the observations of the scanning multichannel microwave radiometer, *Radio Science*, 15: 525-544.